

TELECONNECTIONS BETWEEN INDIAN MONSOON AND SAHEL RAINFALL AND THE MEDITERRANEAN

FABIO RAICICH,^{a,*} NADIA PINARDI^b and ANTONIO NAVARRA^c

^a *CNR, Istituto Sperimentale Talassografico, Trieste, Italy*

^b *Università di Bologna, Corso di Laurea in Scienze Ambientali, Ravenna, Italy*

^c *Istituto Nazionale di Geofisica e Vulcanologia, Bologna, Italy*

Received 8 November 2001

Revised 13 August 2002

Accepted 10 August 2002

ABSTRACT

The teleconnections with Indian monsoon and Sahel rainfall indices are investigated here on an interannual time scale in terms of meteorological and marine dynamics over the Mediterranean area. Sea-level pressure from gridded data sets and from individual stations, together with sea-level data from stations all around the Mediterranean coastlines, are used.

In summer (July–August–September, JAS) the sea-level pressure field over the eastern Mediterranean anticorrelates with the Indian monsoon index (correlation coefficient $C = -0.5$ on average). A Mediterranean pressure index (MPI), defined as the standardized difference between sea-level atmospheric pressure at Mersa Matruh (southeastern Mediterranean) and Marseille (northwestern Mediterranean) stations, anticorrelates with Indian monsoon index even more ($C = -0.68$). The MPI is proportional to the mean geostrophic surface flow field across an imaginary line joining the two stations and turns out to be significantly correlated with the meridional wind component over the eastern Mediterranean, known as the low-level Etesian wind regime. This wind regime represents the inflow surface field into the African inter-tropical convergence zone and, therefore, has an association with the Indian monsoon regime. The ocean response, evident by sea-level anomalies at coastal stations, shows a maximum anticorrelation with Indian monsoon index in late summer and autumn (September–October–November, SON).

The Sahel index anticorrelates with sea-level pressure, with the maximum absolute value in June–July–August. This may be interpreted as a tendency of the Mediterranean sea-level pressure anomalies to precede those of Sahel precipitation, which is characterized by maximum rainfall in July–September. The MPI anticorrelates with Sahel index during and before JAS, indicating that the Etesian wind regime intensity is connected to Sahel rainfall. The sea level again anticorrelates with the Sahel index, with the maximum absolute value in SON, as for the sea-level–Indian monsoon correlation. Copyright © 2003 Royal Meteorological Society.

KEY WORDS: Mediterranean Sea; teleconnections; sea-level pressure; sea level; Indian monsoon rainfall; Sahel rainfall

1. INTRODUCTION

The Mediterranean region appears to be part of global teleconnection patterns emanating from or connecting to the Indian monsoon and Sahel regions. Kraus (1958) was among the first to identify that precipitation over different tropical areas was connected on a decadal time scale. Ward (1992, 1996, 1998) extended this work to interannual time scales by finding significant correlations between Mediterranean meteorological and marine parameters (sea-level atmospheric pressure, surface wind and sea-surface temperature) and Indian monsoon and Sahel rainfall. Rodwell and Hoskins (1996) found that the Indian Monsoon activity can induce a Rossby wave response, which produces an adiabatic descent amplified over the eastern Mediterranean. Thus, it is possible to hypothesize that the Mediterranean area lies in a region of interaction between the Indian monsoon and Sahel atmospheric regimes.

* Correspondence to: Fabio Raicich, CNR, Istituto Sperimentale Talassografico, Viale Romolo Gessi 2, 34123 Trieste, Italy; e-mail: fabio.raicich@itt.ts.cnr.it

The Mediterranean is a boundary region that feels both the dynamics of the tropical circulation cells and the mid-latitude stationary waves. The seasonal cycle is consequently very important, since it regulates the transition from the winter regime, dominated by mid-latitude wave–mean flow interactions, to the summer regime, characterized by the tropical dynamics. The climatological circulation in the Mediterranean region is shown in Figure 1 for the 850 and 500 hPa flow fields. The European Centre for Medium-range Weather Forecast (ECMWF) re-analysis fields (Gibson *et al.*, 1997) were used and averaged over the 1979–93 time period. During winter, the whole Mediterranean is influenced by westerlies, as shown in Figure 1(a), which are strongly modified at the surface by local orography. During summer the westerlies are weaker (Figure 1(b)) and a meridional regime develops, especially over the eastern Mediterranean basin. In the past, this surface flow regime was termed the Etesian wind regime and it clearly connects the eastern Mediterranean area with the sub-Saharan area. At 500 hPa the winds are always westerly, with larger deviations from zonality during summer than in winter, reflecting the surface Etesian regime.

The local vertical circulation can be schematized by streamlines computed from the meridional and vertical velocity field. Ascending branches are connected to convective processes, which may lead to precipitation, whereas descending motion indicates subsidence. The meridional vertical circulation cell here is called the local Hadley cell and it shows a dramatic shift between summer and winter, as shown in Figure 2, indicating a displacement of the convective area from the 0–5°N latitude band to the 15–20°N band. The low-level southern branch of this Hadley cell is composed of a northerly wind regime known as Etesian or Meltemi (Meteorological Office, 1962; hereafter called Etesian), already shown near the surface in Figure 1(b). The African inter-tropical convergence zone (ITCZ) normally positions over the ascending branch of the local Hadley cell connected to the local precipitation maxima during July–August–September (henceforth JAS).

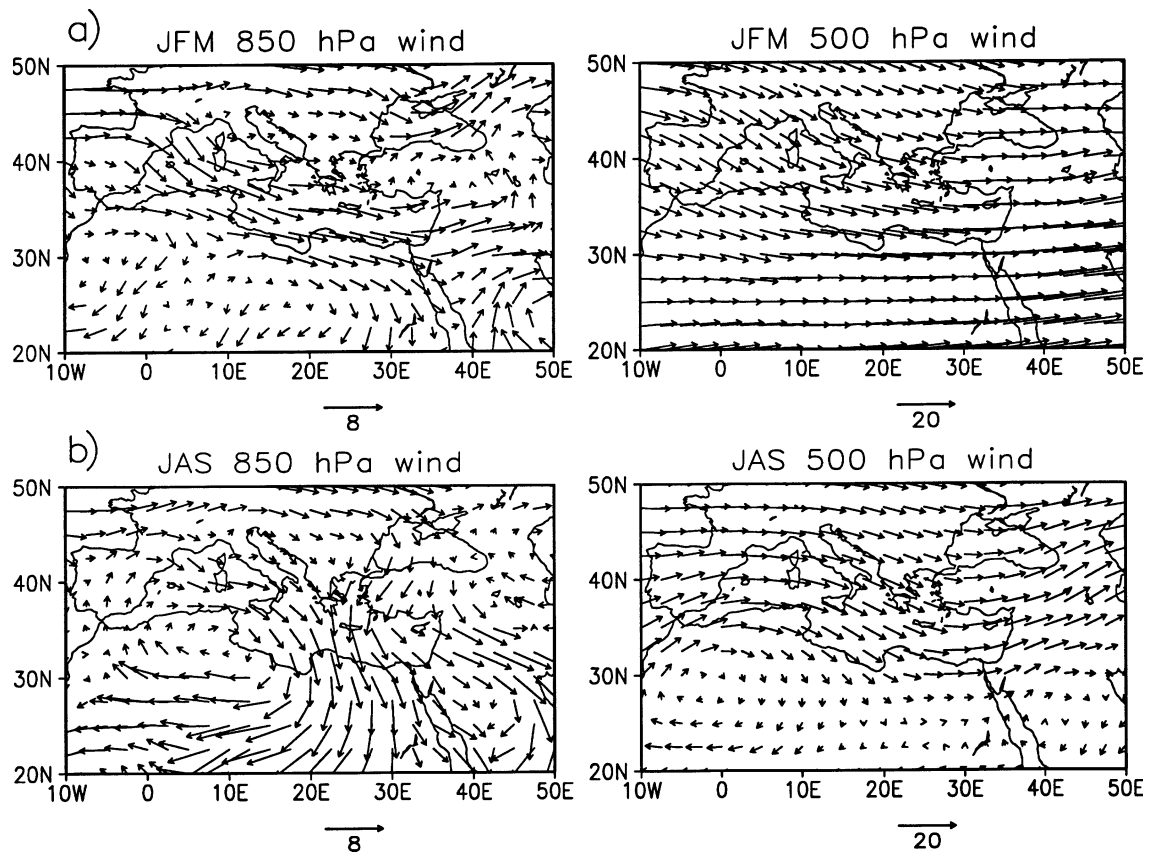


Figure 1. Wind climatologies from ECMWF reanalysis fields at 850 and 500 hPa, for JFM (a) and JAS (b)

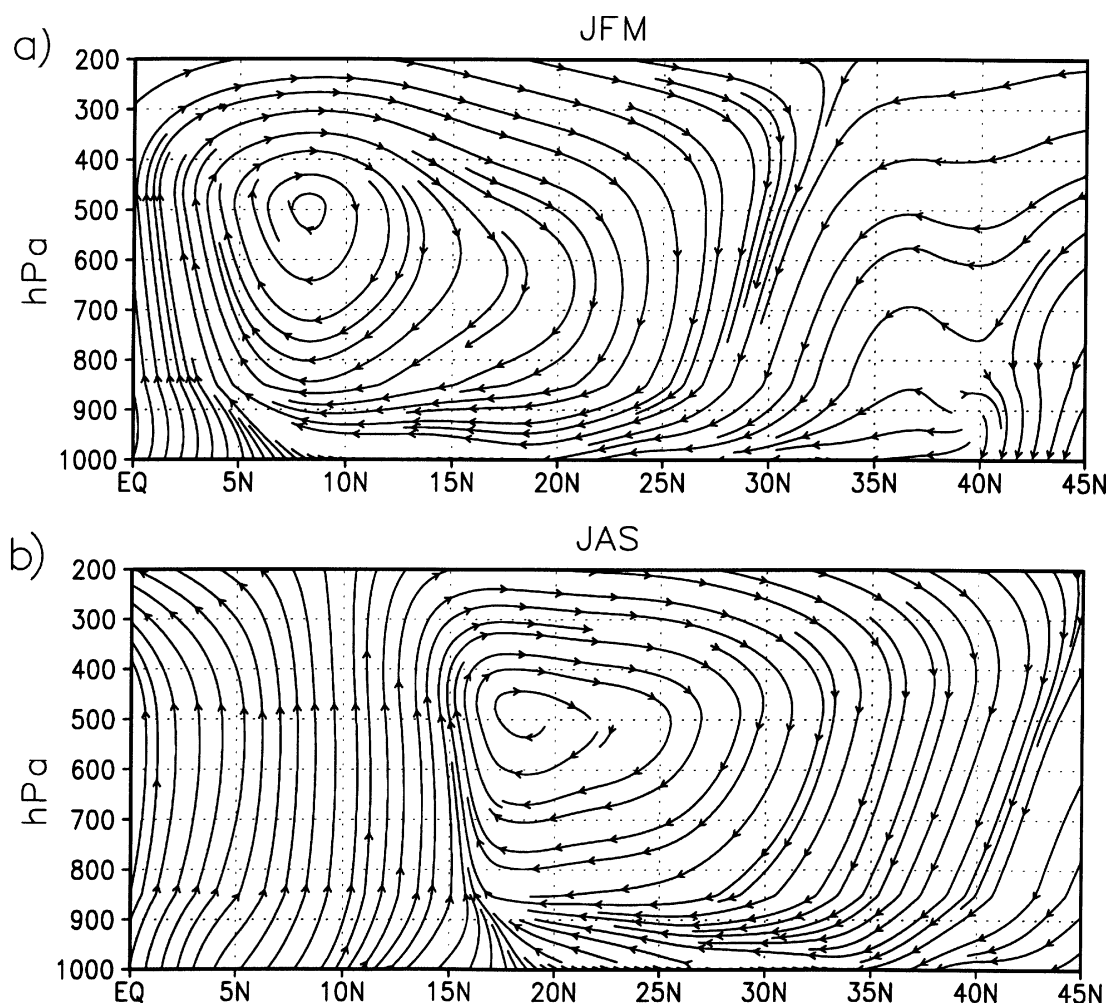


Figure 2. JFM (a) and JAS (b) streamlines obtained from meridional and vertical velocity fields averaged between 15 and 35°E. The lines with arrows (streamlines) indicate only the flow direction, not its intensity

This Hadley cell regime and its seasonal shift is then the basic large-scale physical process that contributes to the Sahel's precipitation variability. Thus, the Mediterranean summer climate seems to be strongly connected to the tropical regime, in particular the low-level flow in the ascending branch of the local Hadley cell.

Ward (1998) found that the precipitation indices for the Indian Monsoon and the Sahel region are correlated on an interannual basis. The correlation coefficient for these data sets is about 0.5 (Figure 3). At the moment, the chain of events that composes the links between the two areas is unclear. In this paper we try to describe the observational evidence that a possible connection is the interannual modulation of the low-level inflow into the ascending branch of the African ITCZ over the eastern Mediterranean region.

Time series of surface data will be used to investigate the teleconnections between Indian monsoon and Sahel rainfall indices and Mediterranean meteorological and marine surface parameters, such as sea-level atmospheric pressure and sea-level elevation. The final aim is to demonstrate that, during the summer, the Mediterranean Sea region is part of a tropical circulation system that connects the Indian monsoon and Sahel areas.

In Section 2 we describe the data sets used, and in Sections 3 and 4 we analyse the correlation fields between the Indian monsoon and the Sahel regions and the Mediterranean respectively. Conclusions in Section 5 will close the paper.

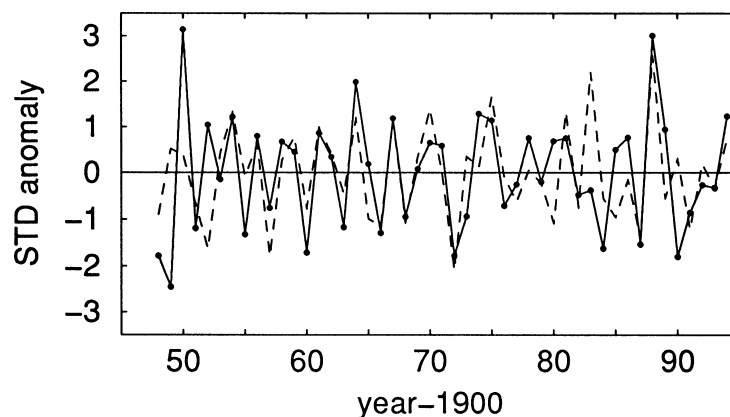


Figure 3. Comparison of high-pass filtered time series of Indian monsoon (dashed line) and Sahel (solid line) indices, computed from JAS precipitation anomalies. Correlation coefficient $C = 0.53$

2. THE DATA SETS

We will use data for the following meteorological and marine parameters: Indian monsoon and Sahel precipitation indices, sea-level pressure and sea-level elevation.

The precipitation indices represent standardized anomalies of total precipitation in JAS for the period 1948–94 and are constructed from the Hulme (1994) data set. The location for the Indian monsoon index is India south of 27.5°N and for the Sahel index it is the region within $12.5\text{--}17.5^{\circ}\text{N}$, $18.75^{\circ}\text{W}\text{--}37.5^{\circ}\text{E}$. A description of such regions can be found in Ward (1998). We limit our analysis to 1948–94, since previous data are affected by uncertainties that reduce the reliability of correlations (Ward, 1998).

We use two sea-level atmospheric pressure data sets. The first consists of gridded $5^{\circ} \times 5^{\circ}$ monthly means (Jackson, 1986). The second is composed of monthly means for selected stations along the coast of the Mediterranean Sea (Figure 4(a)). Such stations are chosen because they lie close to the coast and are represented by long and homogeneous time series; data are taken from the National Climatic Data Center (Vose *et al.*, 1997).

The sea-level elevation data set consists of monthly mean sea levels observed at sea-level gauge stations (Figure 4(b)) and comes from the Permanent Service for Mean Sea Level (Spencer and Woodworth, 1993). All the stations in the western and central Mediterranean are provided with a local reference, which enables us to obtain reliable time series, whereas a local reference is not available for the eastern Mediterranean stations. To obtain at least approximate indications on sea-level variability in the eastern Mediterranean stations, we intercompared the available time series in order to detect outliers and discontinuities. As a result, we retained the time series for Alexandria, which appears to be homogeneous, and a time series consisting of a combination of data for Izmir and Antalya, hereafter named Izmir.

Sea-level atmospheric pressure and sea-level data are processed as follows. Monthly standardized anomalies are computed by removing the climatological means from the original data and dividing the result by the climatological standard deviations. Then, 3-month mean anomalies are obtained by averaging the standardized anomalies of three consecutive months, namely January–February–March (henceforth JFM), February–March–April (FMA), and so on, up to December and January–February of the following year (DJF). When one or more monthly anomalies are missing, the related 3-month anomaly is also set to missing. Time series are thus formed for all the 3-month periods.

In this work we study the interannual variability signal and, therefore, all time series are high-pass filtered by means of the filtering technique developed by Ng and Young (1990). The 50% cut-off frequency is set at about 11.25 years. All the results described in this paper concern the analysis of the high-frequency (interannual) components of the time series of standardized 3-month anomalies. The statistical significance of correlations is set at the 95% confidence level. Note that the filtering procedure also removes the effect of possible slow vertical ground displacements on sea-level time series.

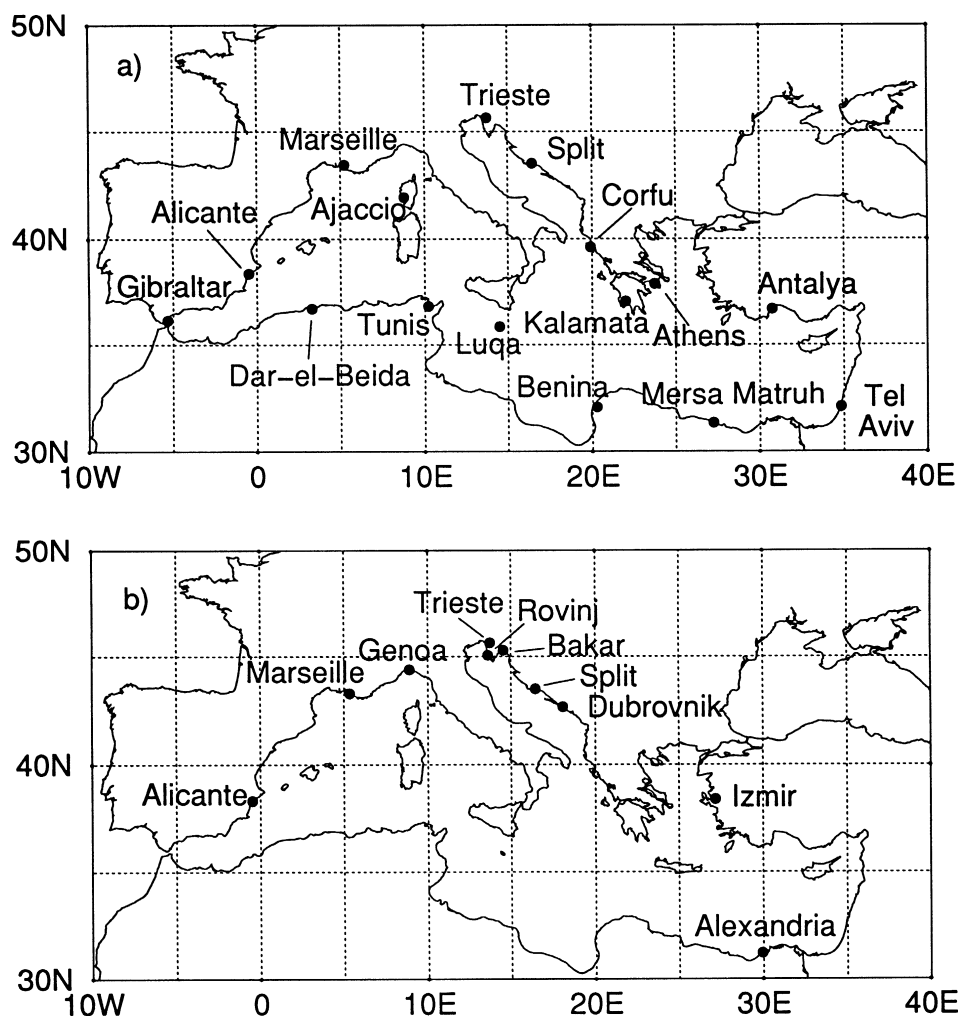


Figure 4. Location of sea-level atmospheric pressure (a) and sea level (b) stations adopted in this work

3. THE INDIAN MONSOON — MEDITERRANEAN TELECONNECTION

3.1. Sea-level atmospheric pressure

Sea-level atmospheric pressure–Indian monsoon teleconnection patterns are shown in Figure 5 for time lags from -1 to $+2$ months, that is from June–July–August (JJA) to September–October–November (SON). The maps show correlation coefficients of sea-level atmospheric pressure with the Indian monsoon index; shaded areas are significant at the 95% confidence level.

In the Mediterranean area, significant anticorrelation is seen over the Levantine Basin in JAS, as a part of a large structure extending over the Middle East, northeast Africa and the Arabian peninsula, where the maximum anticorrelation is found. The negative sign means that an increased Indian monsoon precipitation corresponds to lower atmospheric pressure. Over the Mediterranean Sea the correlation coefficient C is lower than -0.5 close to Israel and the Sinai peninsula. Significant anticorrelation was already found by Ward (1996), with a different atmospheric pressure data set. A positive correlation area is found over the western basin with maximum development 2 months later (SON). The pressure anomalies in those regions are potentially important to modulate the interannual variability of the wind systems in the eastern Mediterranean (Figure 1(b)). The seasonal cycle shows the presence of intense northerly winds in summer (the Etesians)

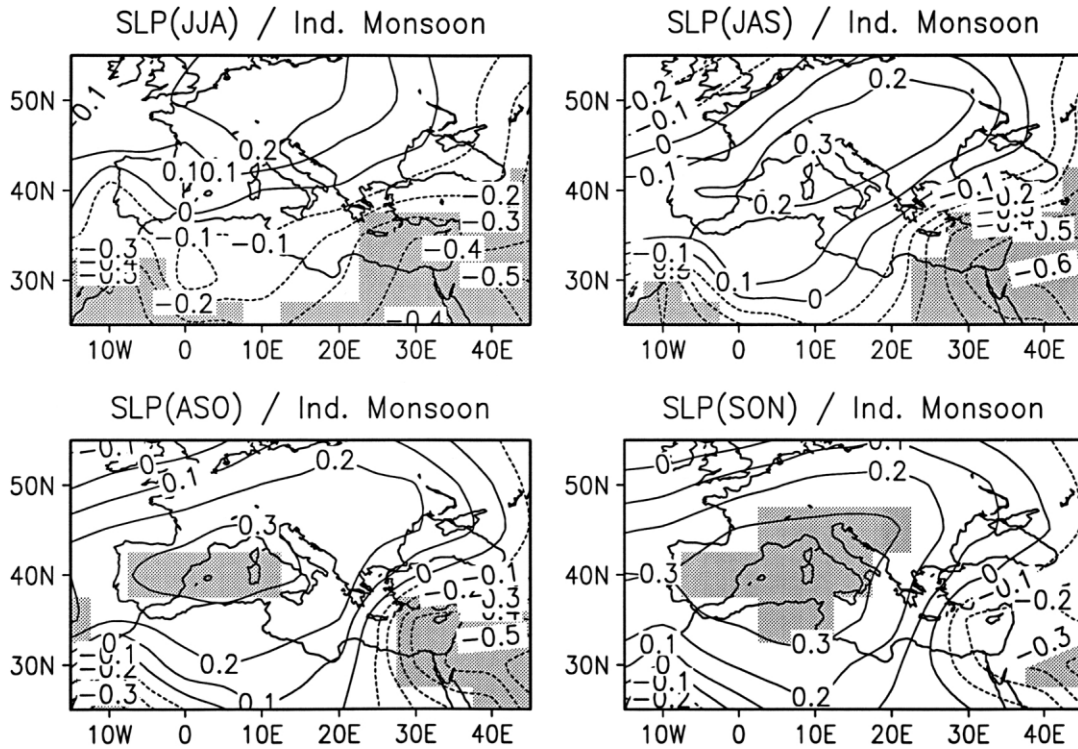


Figure 5. Maps of correlation coefficients between Indian monsoon index, defined for JAS, and sea-level atmospheric pressure for JJA (upper-left panel), JAS (upper right), ASO (lower left) and SON (lower right). The corresponding time lags of sea-level atmospheric pressure relative to Indian monsoon index are -1 to $+2$ months. Correlations significant at the 95% confidence level are shaded

that are the geostrophic component of the flow field at the western edge of the low-pressure area over the Middle East.

The results obtained from station data are consistent with those from gridded data previously outlined. Anticorrelation, peaked in JAS, is found for the stations in the Levantine Basin, represented in Figure 6(a) by Mersa Matruh, whereas for stations in the western Mediterranean and the Adriatic Sea, represented in Figure 6(b) by Ajaccio, the correlation is positive and peaked in SON. In between, that is in the Ionian and Aegean Seas, there is no significant correlation. Figure 7 shows the overall correlation between sea-level atmospheric pressure measured at stations and the Indian monsoon index for JAS (Figure 7(a)) and SON (Figure 7(b)).

Figure 8 shows the comparison between the time series of the Indian monsoon index and standardized sea-level atmospheric pressure difference between Mersa Matruh and Marseille stations in JAS. This standardized pressure difference, hereafter called the Mediterranean pressure index (MPI), is based on the sea-level pressure difference, between one station in the eastern Mediterranean and one in the western Mediterranean, that is highest anticorrelated with Indian monsoon ($C = -0.68$). The time series of JAS pressure difference Mersa Matruh–Marseille is shown in Figure 9; its mean value is -4.4 ± 1.0 hPa. The MPI sign is chosen so that a positive pressure gradient is related to a positive geostrophic wind component. In the coordinate framework, where x is positive eastwards and y is positive northwards, the climatological negative pressure difference Mersa Matruh–Marseille is consistently related to climatological northerly winds. The MPI is proportional to the mean geostrophic flow field orthogonal to a line joining the two stations. Furthermore, a significant correlation ($C = 0.68$) is found for the period 1948–94 between the MPI and the average meridional wind component over the eastern Mediterranean (30 – 40° N, 20 – 35° E, from National Centers for Environmental Prediction reanalysis). It is known that the Etesian regime prevails in summer with a large-amplitude meridional component (Figure 1(b)); thus the MPI can reasonably represent variability in the Etesian wind regime.

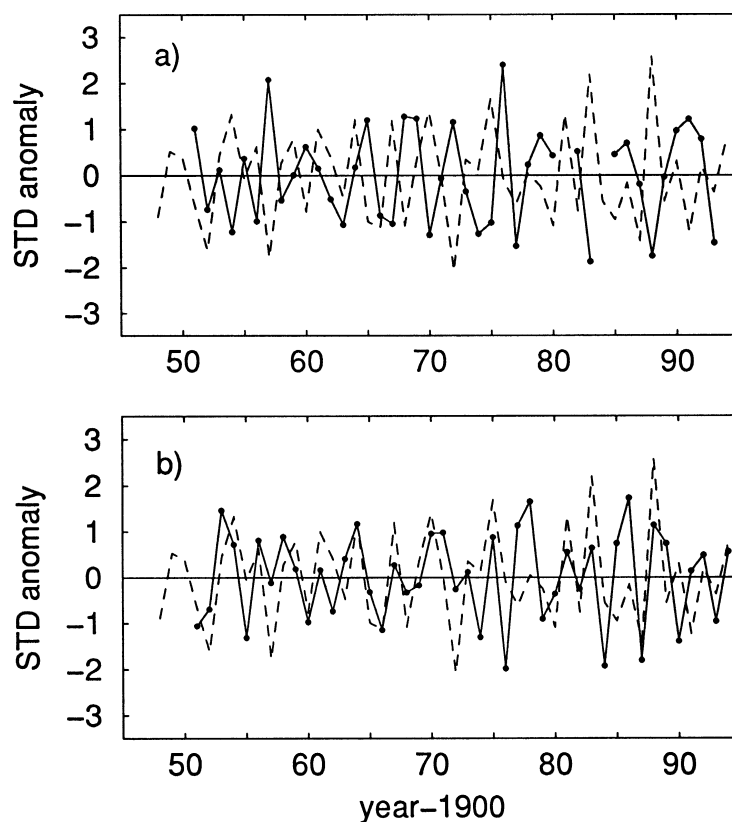


Figure 6. Comparison of time series of Indian monsoon index (dashed lines) and sea-level atmospheric pressure (solid lines) at Mersa Matruh in JAS (a) and Ajaccio in SON (b)

Higher precipitation over India then corresponds to lower MPI, i.e. lower sea-level pressure in the eastern Mediterranean and/or higher sea-level pressure in the western Mediterranean, which in turn could mean an intensified Etesian wind regime (measured here as the Mersa Matruh–Marseille pressure difference).

In conclusion, the Indian Monsoon index and surface pressure signals over the eastern Mediterranean are anticorrelated during JAS. We also find maximum anticorrelation between the Indian monsoon index and MPI, indicating a connection between the low-level inflow into the northeast African local Hadley cell and the Indian monsoon regime.

3.2. Sea-level elevation

With the exception of Alicante, Dubrovnik and Izmir, the sea level is significantly anticorrelated with the Indian Monsoon precipitation index, with extreme values in SON (Figure 10). Concerning the stations in the northern part of the basin (Marseille, Genoa and those in the northern Adriatic), we also recall that the sea-level atmospheric pressure–Indian monsoon correlation peaked in SON, with a positive sign (Figure 7).

It is known that surface pressure and sea level may be anticorrelated by the static inverse barometer effect, which can be written as $\rho_0 g \Delta \eta = -\Delta p_a$ (e.g. Bowden, 1983), where ρ_0 is sea water density, assumed to be constant along the water column, g is acceleration due to gravity, $\Delta \eta$ is sea-level anomaly and Δp_a is atmospheric pressure anomaly. In our time series, significant anticorrelation between atmospheric pressure and sea level is usually found in all months, as shown in Table I, with the exception of the eastern Mediterranean stations (Izmir and Alexandria). The absolute value of the correlation coefficient reaches its minimum in JAS, whereas the maximum is observed in winter or early spring. The relatively low correlation in SON indicates

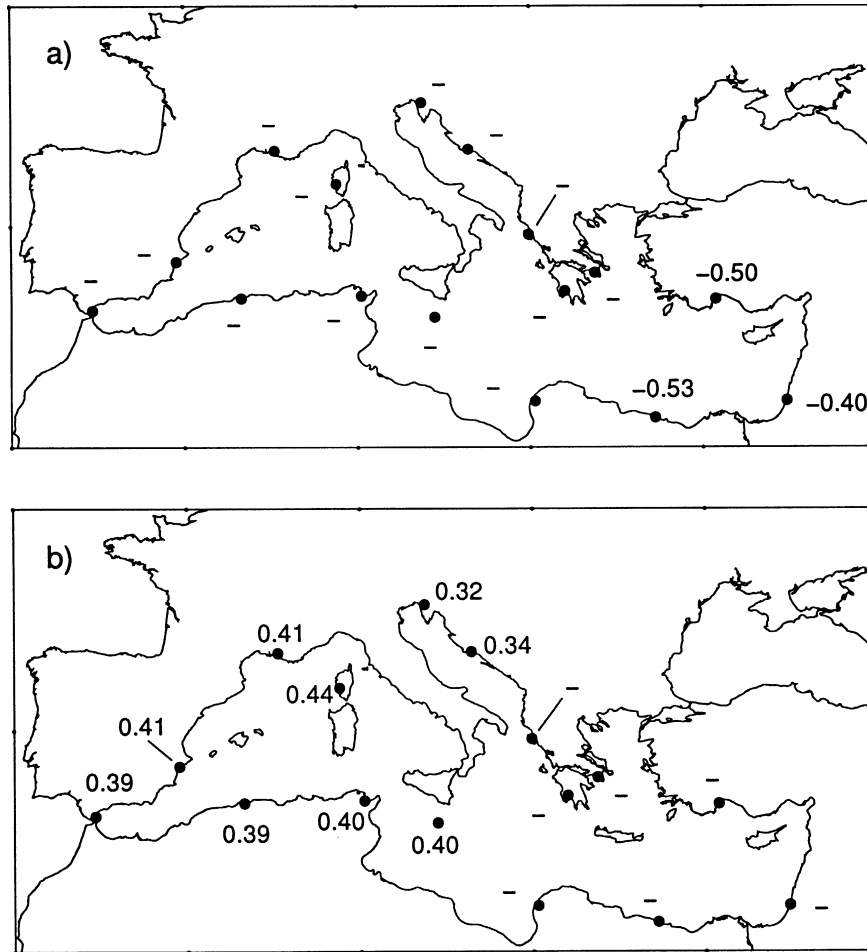


Figure 7. Correlation coefficients for teleconnections of Indian monsoon with sea-level atmospheric pressure from station data in JAS (a) and SON (b). Dashes indicate non-significant correlations at the 95% confidence level

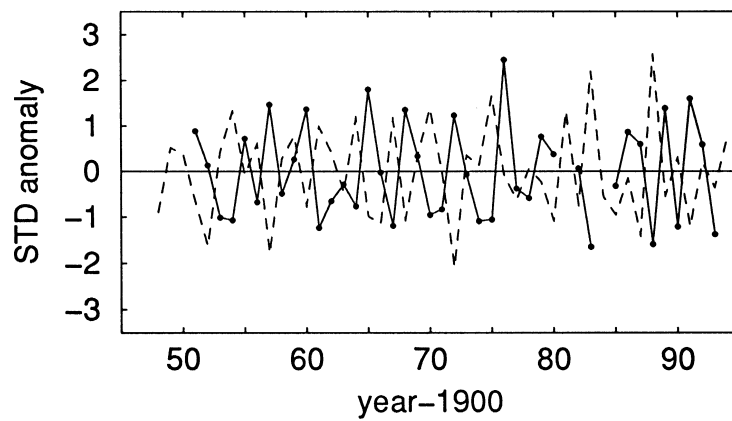


Figure 8. Comparison of time series of Indian monsoon index (dashed line) and the MPI (defined as the sea-level atmospheric pressure difference between Mersa Matruh and Marseille) in JAS (solid line). $C = -0.68$

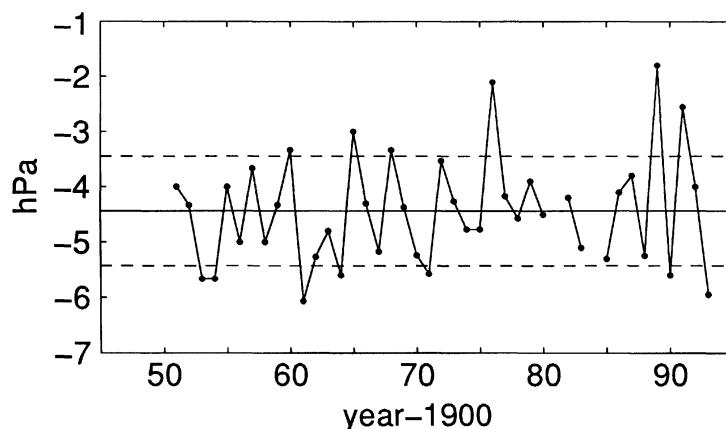


Figure 9. Time series of observed sea-level atmospheric pressure difference between Mersa Matruh and Marseille in JAS. The mean is -4.4 ± 1.0 hPa. The horizontal lines represent the mean (solid) and mean \pm standard deviation (dashed)

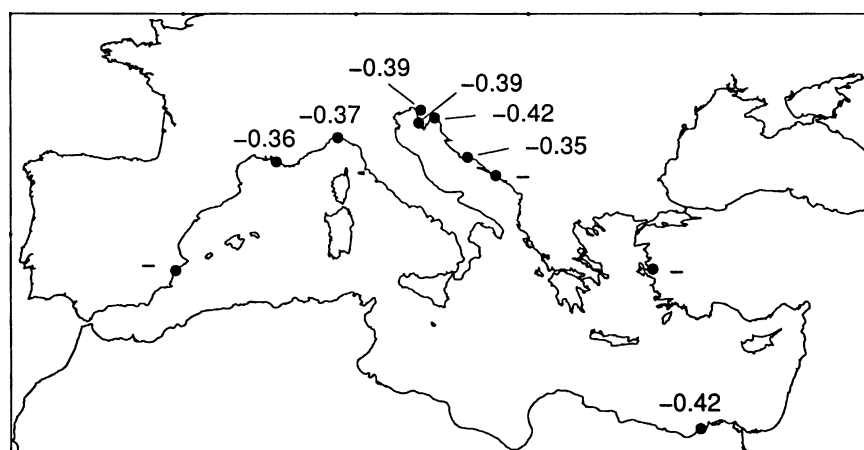


Figure 10. Correlation coefficients for teleconnections of Indian monsoon with sea level in SON. Dashes indicate non-significant correlations at the 95% confidence level

that the sea-level modulation due to the inverse barometer effect is not the dominant process, and that a notable part of sea-level variability is connected to ocean baroclinic processes, such as heat storage distribution and wind-driven currents. The significant anticorrelation between sea level and the Indian monsoon index should then be interpreted also in terms of those processes, but to elucidate them we would need long time series of temperature and salinity data at the sea-level station locations, which are not available.

In conclusion, we found that during SON the sea-level anomalies at coastal stations are anticorrelated with the Indian monsoon index and sea-level pressure. This may mean that the ocean has a memory mechanism that stores surface heat flux changes induced by the Indian monsoon regime in JAS, making them evident 2 months later.

Alternatively, it may only be a simple response to atmospheric pressure effects, which exhibit maximum positive correlation with Indian monsoon in SON over the western and northern Mediterranean regions. The reason why the eastern Mediterranean stations do not exhibit significant anticorrelation in JAS and SON requires further studies. An analysis of the ocean heat storage changes could shed light on this complicated issue.

Table I. Correlation between sea level (SL) and sea-level pressure (SLP) at selected stations. NS indicates non-significant correlation

Period	Trieste	Split	Marseille	Alicante	Izmir	Alexandria
JFM	-0.88	-0.80	-0.87	-0.89	NS	-0.35
FMA	-0.83	-0.77	-0.89	-0.76	NS	NS
MAM	-0.72	-0.69	-0.78	-0.73	NS	NS
AMJ	-0.62	-0.65	-0.72	-0.72	NS	NS
MJJ	-0.59	-0.59	-0.51	-0.59	NS	NS
JJA	-0.59	-0.54	NS	-0.58	NS	NS
JAS	-0.52	-0.39	NS	-0.64	NS	NS
ASO	-0.58	-0.41	NS	-0.61	NS	NS
SON	-0.77	-0.74	-0.55	-0.67	NS	-0.37
OND	-0.82	-0.83	-0.61	-0.68	-0.62	-0.53
NDJ	-0.85	-0.79	-0.62	-0.80	-0.64	-0.59
DJF	-0.91	-0.73	-0.64	-0.89	-0.52	-0.58

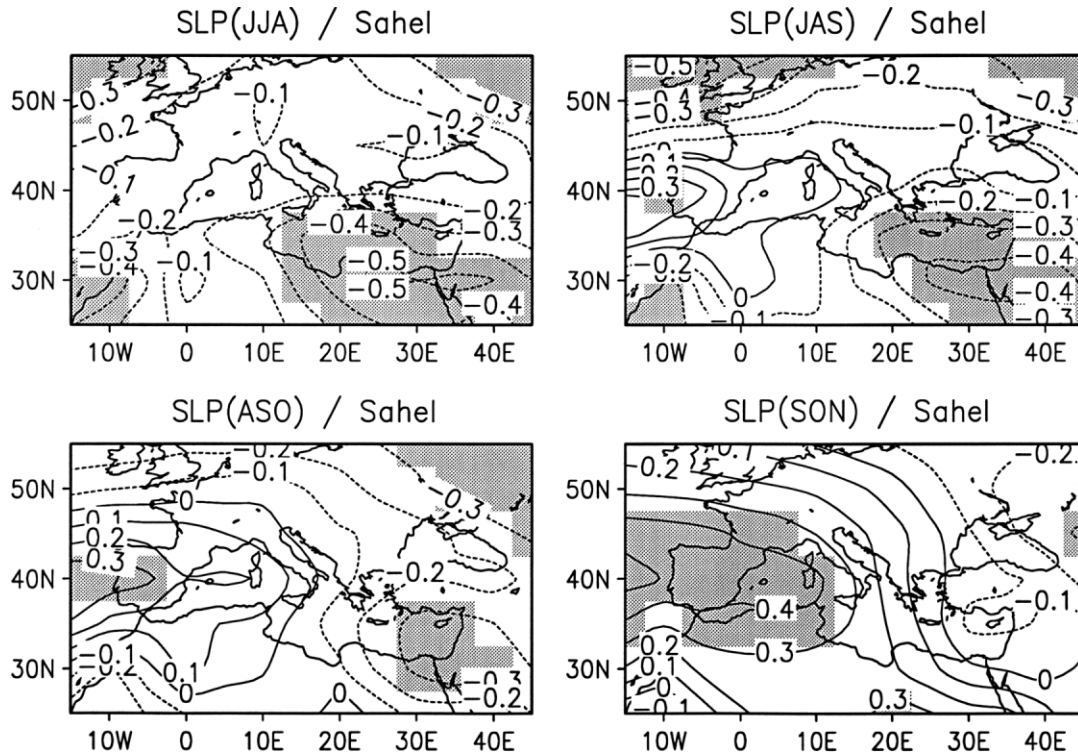


Figure 11. Maps of correlation coefficients between Sahel index, defined for JAS, and sea-level atmospheric pressure for JJA (upper-left panel), JAS (upper right), ASO (lower left) and SON (lower right). The corresponding time lags of sea-level atmospheric pressure relative to Sahel index are -1 to $+2$ months. Correlations significant at the 95% confidence level are shaded

4. THE SAHEL–MEDITERRANEAN TELECONNECTION

4.1. Sea-level atmospheric pressure

Sea-level atmospheric pressure–Sahel teleconnection patterns are shown in Figure 11 for time lags from -1 to $+2$ months. Two features can be recognized: the southeastern part of the basin exhibits an anticorrelation

with the Sahel precipitation index which peaks in JJA, and a maximum positive correlation over the western Mediterranean in SON. The maximum anticorrelation appears to occur slightly earlier than the peak rainfall season in JAS, according to the index definition, although a 1 month time lag cannot be resolved in our analysis. The anticorrelation implies that lower atmospheric pressure in northeast Africa and the eastern Mediterranean is related to higher precipitation in the Sahel region. This result for JAS was also found by Ward (1992, 1996), but here we find that the maximum is in JJA. In SON, i.e. 2 months later than the peak rainfall season, the whole western Mediterranean, together with northwest Africa, becomes correlated with the Sahel index. This indicates that, on a statistical basis, a more rainy summer in the Sahel is followed by a higher atmospheric pressure distribution in the western Mediterranean in the autumn season.

The picture emerging from the analysis of sea-level pressure station data is consistent with the same analysis done with the gridded sea-level pressure data. The eastern Mediterranean stations (Mersa Matruh), except the Adriatic Sea, exhibit negative correlations that peak in JJA (Figure 12(a)), whereas those in the western basin (Ajaccio) are positively correlated, with peaks in SON (Figure 12(b)). Figure 13 summarizes the overall correlation between atmospheric sea-level pressure measured at stations and the Sahel index for JJA (Figure 13(a)) and SON (Figure 13(b)).

In Figure 14 we compare the time series of the Sahel index and MPI in JAS. Significant anticorrelation exists, with $C = -0.47$. The MPI exhibits maximum anticorrelation with the Sahel index in JAS, but significant anticorrelation with almost the same strength also exists previously, namely in MJJ and JJA (Table II). Since the MPI represents the Etesian surface wind regime, the latter can be thought of as a component of the Sahel circulation regimes.

It is unclear which physical mechanisms are behind the MPI–Sahel index anticorrelation. However, the results may be related to the enhancement of the low-level convergence into the summer African ITCZ.

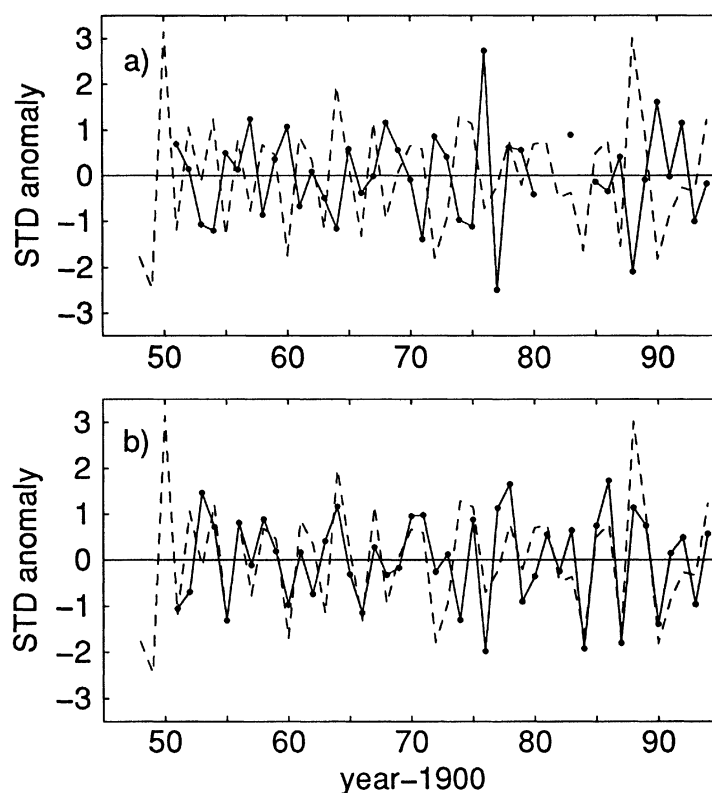


Figure 12. Comparison of time series of Sahel index (dashed lines) and sea-level atmospheric pressure (solid lines) at Mersa Matruh in JJA (a) and Ajaccio in SON (b)

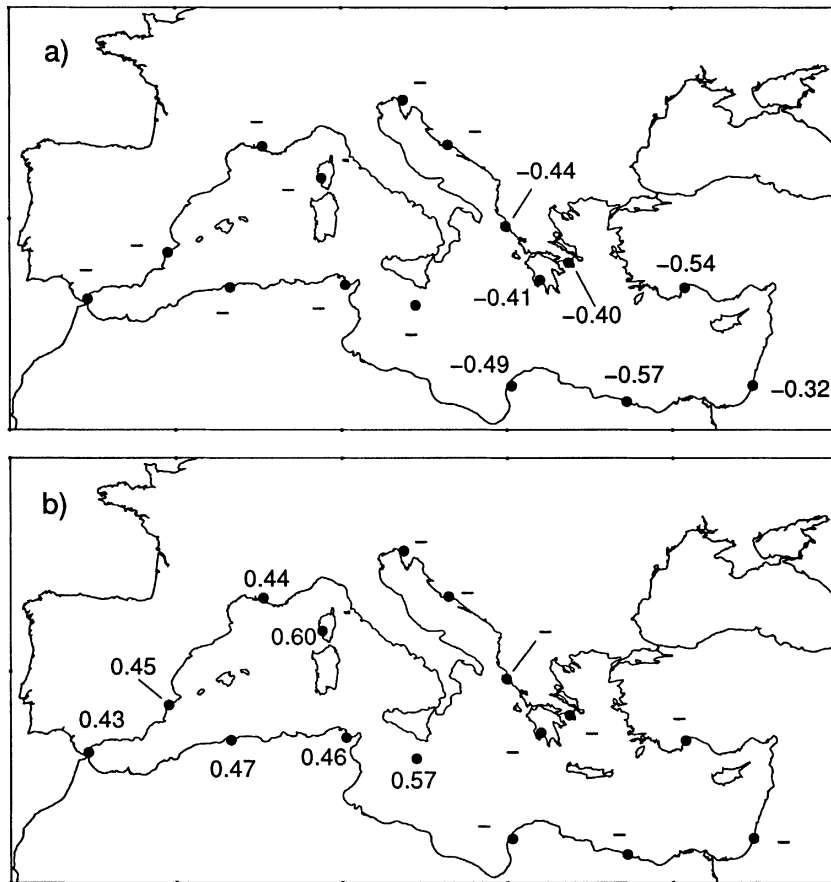


Figure 13. Correlation coefficients for teleconnections of Sahel with sea-level atmospheric pressure from station data in JAS (a) and SON (b). Dashes indicate non-significant correlations at the 95% confidence level

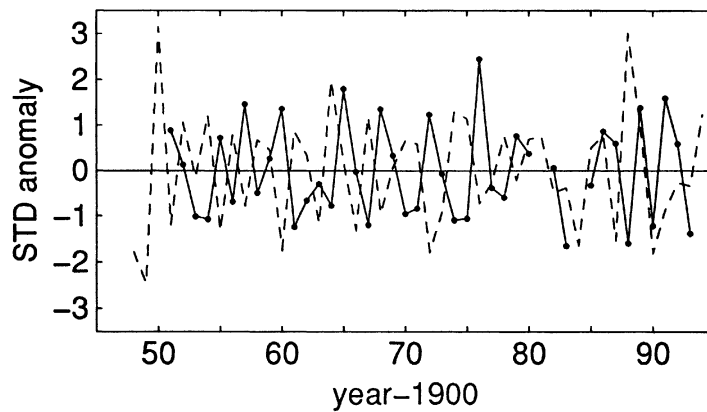


Figure 14. Comparison of time series of Sahel index (dashed line) and the MPI (defined as the sea-level atmospheric pressure difference between Mersa Matruh and Marseille) in JAS (solid line). $C = -0.47$

4.2. Sea-level elevation

Significant anticorrelation is found between sea level and the Sahel index at all stations, with peak values in SON (Figure 15), as was the case for sea-level–Indian monsoon teleconnection. Anticorrelation is particularly

Table II. Correlation between MPI and Indian monsoon and Sahel indices. NS indicates non-significant correlation

Period	Indian monsoon	Sahel
MJJ	-0.44	-0.43
JJA	-0.54	-0.46
JAS	-0.68	-0.47
ASO	-0.60	-0.36
SON	-0.62	-0.35
OND	-0.40	NS

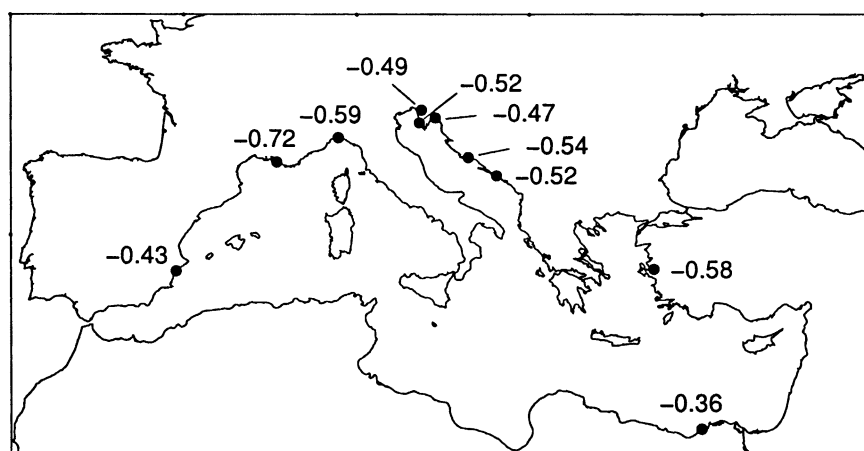


Figure 15. Correlation coefficients for teleconnections of Sahel with sea level in SON. Dashes indicate non-significant correlations at the 95% confidence level

notable in the northwest Mediterranean, with $C = -0.72$ at Marseille. A significant anticorrelation is seen this time also for Izmir ($C = -0.58$). The higher absolute value of anticorrelation between sea-level and Sahel index fluctuations, compared with those for sea level and Indian monsoon index, contributes to strengthen the evidence that the Mediterranean circulation conditions may be strongly correlated with Sahel rainfall anomalies. It is possible to speculate that the process may be a coupled process between the Mediterranean Sea and the Sahel, but we do not have conclusive evidence to this end.

In order to understand which mechanism is underpinned by such correlations, adequate time series of subsurface temperature and salinity data at the sea-level stations should be analysed, but they are not available. As discussed before, the sea level could mirror a mechanism related to subsurface heat storage changes which manifests itself 2 months later than the JAS maximum rainfall season. The sea-level–Sahel index anticorrelation in SON confirms that a memory mechanism is active in the Mediterranean ocean basin.

5. CONCLUSIONS

From this analysis we conclude that significant correlations exist between both the Indian monsoon and Sahel rainfall regimes and sea-level atmospheric pressure and elevation in the Mediterranean area, with different characteristics for western and eastern Mediterranean basins.

Concerning sea-level atmospheric pressure, the correlations with Indian monsoon and Sahel show different structures. The eastern basin exhibits negative correlations with both precipitation indices. Whereas the anticorrelation with the Indian monsoon index is simultaneous (in JAS), the Sahel index is anticorrelated

with atmospheric pressure also in JJA. The western basin exhibits maximum positive correlation in SON, i.e. 2 months later than the peak precipitation anomalies over both the Indian monsoon and Sahel regions. The nature of this lagged relation is unclear, and further investigation is required to assess its reliability.

The maxima in the correlation between sea-level and precipitation indices always occur in SON, and generally concern the northern Mediterranean Sea. These areas of the Mediterranean Sea seem to respond quite regularly to positively correlated pressure anomalies developing 2 months after the Indian monsoon and Sahel maximum precipitation anomalies. The northern Mediterranean areas are outside the direct range of influence of the descending branch of the Hadley circulation, so the mechanism for this relation must be indirect.

We found that the maximum correlation with Indian monsoon and Sahel indices during summer can be extracted from the MPI, which, in turn, is used to measure the strength of the low-level branch of the inflow into the local Hadley cell over the Mediterranean Sea. This surface wind regime is simultaneously (in JAS) anticorrelated with both Indian monsoon and Sahel indices. Correlation with the Sahel index of the same strength is found before JAS; thus, the MPI might represent a dynamical mechanism connected to Sahel rainfall anomalies and the Etesian wind regime strength. This may indicate an active role of the Mediterranean surface regimes in determining the Sahel precipitation system.

This work shows that the Mediterranean Sea area takes part in the tropical circulation regime developing during summer over the African region. The low-level branch of the local Hadley cell is related to the Etesian wind regime, which is associated with negative values of the MPI. The Indian monsoon circulation is clearly correlated to the low-pressure distribution over the Middle East. The geostrophic component of the Etesian wind regime is connected to the strength of this low-pressure system, and this could explain the high anticorrelation between the MPI and the Indian monsoon index.

The physical mechanism explaining the MPI–Sahel index anticorrelation is still unknown, but it may involve the enhancement of the low-level convergence into the summer African ITCZ and subsidence variations arising from the interannual variability of the Sahelian ITCZ.

ACKNOWLEDGEMENTS

We thank Professor K. Miyakoda and Dr N. Ward for discussions and suggestions. Thanks also go to Ms T. Basnett (UK Meteorological Office) and Dr V. Moron for making the gridded atmospheric pressure data available. This work has been partly funded by ENEA contract 'Programma di Ricerca Applicata Settore Ambiente Mediterraneo'.

REFERENCES

- Bowden KF. 1983. *Physical Oceanography of Coastal Waters*. Ellis Horwood Ltd: Chichester, UK.
- Gibson JK, Källberg P, Uppala S, Hernandez A, Nomura A, Serrano E. 1997. ERA Description. ECMWF Reanalysis Project Report 1.
- Hulme M. 1994. Validation of large-scale precipitation fields in general circulation models. In *Global Precipitation and Climate Change*, Desbois M, Desalmand F (eds). Springer-Verlag: Berlin, Heidelberg; 387–406.
- Jackson M. 1986. Operational Superfiles in Met.O.13. Met.O.13 Technical Note 25.
- Kraus EB. 1958. Recent climatic changes. *Nature* **181**: 666–668.
- Meteorological Office. 1962. *Weather in the Mediterranean*, vol. I. M.O. 391, HMSO: London.
- Ng CN, Young PC. 1990. Recursive estimation and forecasting of non-stationary time-series. *Journal of Forecasting* **9**: 173–204.
- Rodwell MJ, Hoskins BJ. 1996. Monsoons and the dynamic of deserts. *Quarterly Journal of the Royal Meteorological Society* **122**: 1385–1404.
- Spencer NE, Woodworth PL. 1993. Data holdings of the Permanent Service for Mean Sea Level (November 1993). Permanent Service for Mean Sea Level, Bidston, Birkenhead.
- Vose RS, Schmoyer RL, Steurer PM, Peterson TC, Heim R, Karl TR, Eischeid J. 1992. The Global Historical Climatology Network: long-term monthly temperature, precipitation, sea level pressure, and station pressure data. ORNL/CDIAC-53, NDP-041. Carbon Dioxide Information Analysis Center, Oak Ridge National Laboratory, Oak Ridge, Tennessee.
- Ward MN. 1992. Provisionally corrected surface wind data, worldwide ocean–atmosphere surface fields and Sahelian rainfall variability. *Journal of Climate* **5**: 454–475.
- Ward MN. 1996. Local and remote climate variability associated with east Mediterranean sea-surface temperature anomalies. In *Mediterranean Forecasting*. European Science Foundation: Strasbourg.
- Ward MN. 1998. Diagnosis and short-lead time prediction of summer rainfall in tropical North Africa at interannual and multidecadal timescales. *Journal of Climate* **11**: 3167–3191.